Lepke, S., Fasold, H., Pring, M., & Passow, H. (1976) *J. Membr. Biol. 29*, 147-177.
Mikkelson, A., & Elgsaeter, A. (1978) *Biochim. Biophys. Acta 536*, 245-251.
Mikkelson, A., & Elgsaeter, A. (1981) *Biochim. Biophys. Acta 668*, 74-80.
Mühlebach, T., & Cherry, R. J. (1985) *Biochemistry 24*, 975-983.
Nigg, E. A., & Cherry, R. J. (1979) *Biochemistry 18*, 3457-3465.
Nigg, E. A., & Cherry, R. J. (1980) *Proc. Natl. Acad. Sci. U.S.A. 77*, 4702-4706.
Ohanian, V., & Gratzer, W. B. (1984) *Eur. J. Biochem. 144*, 375-379.
Podgorski, A., & Elbaum, D. (1985) *Biochemistry 24*, 7871-7876.
Ralston, G. B. (1978) *J. Supramol. Struct. 8*, 361-373.
Shotton, D. M., Burke, D. E., & Branton, D. (1979) *J. Mol. Biol. 131*, 303-329.
Speicher, D. W., & Marchesi, V. T. (1982) *J. Cell. Biochem. 18*, 471-482.
Speicher, D. W., & Marchesi, V. T. (1984) *Nature 311*, 177-180.
Tsuji, A., Kawasaki, K., Ohnishi, S., Merkle, H., & Kusumi, A. (1988) *Biochemistry 27*, 7447-7452.
Tyler, J. M., Reinhardt, B. N., & Branton, D. (1980) *J. Biol. Chem. 255*, 7034-7039.
Ungewickell, E., & Gratzer, W. B. (1978) *Eur. J. Biochem. 88*, 379-385.
Yoshimura, H., Nishio, T., Mihashi, K., Kinosita, K., Jr., & Ikegami, A. (1984) *J. Mol. Biol. 179*, 453-467.

Rotational Dynamics of the Ca-ATPase in Sarcoplasmic Reticulum Studied by Time-Resolved Phosphorescence Anisotropy†

Woubalem Birmachu and David D. Thomas*
Department of Biochemistry, University of Minnesota Medical School, Minneapolis, Minnesota 55455
Received August 7, 1989; Revised Manuscript Received December 20, 1989

ABSTRACT: We have investigated the microsecond rotational motions of the Ca-ATPase in rabbit skeletal sarcoplasmic reticulum (SR), by measuring the time-resolved phosphorescence anisotropy of erythrosin 5-isothiocyanate (ERITC) covalently and specifically attached to the enzyme. Over a wide range of solvent conditions and temperatures, the phosphorescence anisotropy decay was best fit by a sum of three exponentials plus a constant term. At 4 °C, the rotational correlation times were $\phi_1 = 13 \pm 3$ μs, $\phi_2 = 77 \pm 11$ μs, and $\phi_3 = 314 \pm 23$ μs. Increasing the solution viscosity with glycerol caused very little effect on the correlation times, while decreasing the lipid viscosity with diethyl ether decreased the correlation times substantially, indicating that the decay corresponds to rotation of the protein within the membrane, not to vesicle tumbling. The normalized residual anisotropy (A_∞) is insensitive to viscosity and temperature changes, supporting the model of uniaxial rotation of the protein about the membrane normal. The value of A_∞ (0.20 ± .02) indicates that each of the three decay components can be analyzed as a separate rotational species, with the preexponential factor A_i equal to 1.25× the mole fraction. An empirically accurate measurement of the membrane lipid viscosity was obtained, permitting a theoretical analysis of the correlation times in terms of the sizes of the rotating species. At 4 °C, the dominant correlation time (ϕ_3) is too large for a Ca-ATPase monomer, strongly suggesting that the enzyme is primarily aggregated (oligomeric). From 4 to 20 °C, A_3 decreases markedly (0.43 to 0.15) while A_2 increases (0.14 to 0.40), suggesting a transition to a more mobile (less aggregated) species. At 20 °C, the dominant correlation time (ϕ_2) has a value most consistent with a Ca-ATPase dimer, but a monomer is also possible. Above 20 °C, A_2 decreases in favor of A_1, which has a correlation time (ϕ_1) most consistent with a monomer. Arrhenius plots of protein rotational rates (inverse correlation times) are linear, indicating no abrupt change in protein shape or lipid viscosity. In contrast, the van't Hoff plots of the apparent protein–protein dissociation constants (A_2/A_3 and A_1/A_2) exhibit dramatic slope changes in the range of 18–23 °C, correlating well with changes in the energetics of Ca-ATPase activity and its proposed protein conformational transition. We propose that ATPase monomers and oligomers are in a temperature-dependent equilibrium, with monomers and dimers predominating above 20 °C and higher oligomers predominating at lower temperatures. These results support the hypothesis that protein–protein interaction plays an important role in determining Ca-ATPase activity.

An understanding of the molecular mechanism of active calcium transport in sarcoplasmic reticulum (SR)[1] requires direct information about the molecular dynamics of the Ca-ATPase. One of the fundamental problems that has yet to be resolved is the quaternary structure of the functional ATPase. Protein–protein interactions have been proposed to play an important role in the function of the enzyme. Early observations that only half of the ATPase proteins were capable of forming phosphoenzyme were interpreted as suggesting that

† This work was supported by grants to D.D.T. from NIH (GM27906 and RR01439) and a grant to W.B. from the American Heart Association. D.D.T. was supported by an Established Investigatorship, and W.B. was supported by a Postdoctoral Fellowship, both from the American Heart Association.

[1] Abbrevations: ERITC, erythrosin 5-isothiocyanate; DMF, dimethylformamide; DMPC, dimyristoylphosphatidyl choline; 5- and 12-SASL, *N*-oxy-4′,4′-dimethyloxazolidine derivatives of stearic acid; MOPS, 3-(*N*-morpholino)propanesulfinic acid; ST-EPR, saturation transfer electron paramagnetic resonance; SR, sarcoplasmic reticulum.

0006-2960/90/0429-3904$02.50/0

the functional unit of the ATPase is a dimer (Martonosi et al., 1974). Since monomers in detergent-solubilized preparations can undergo essentially all of the partial reactions of the membrane-bound enzyme (Andersen & Vilsen, 1985; Martins & DeMeis, 1985; McIntosh & Ross, 1988), an oligomeric association may not be required. In addition, reconstituted ATPase preparations with very high lipid-to-protein ratios exhibit kinetics identical with native SR preparations (Vilsen & Andersen, 1987). Nonetheless, the ATPase shows a strong tendency to aggregate even in detergent solutions, and it occurs in an equilibrium distribution of monomers and dimers in nonionic detergents such as $C_{12}E_8$ (Silva & Verjovski-Almeida, 1985).

Many physical methods have been used to investigate the quaternary structure of the functional unit of the Ca-ATPase. X-ray and neutron diffraction results (Herbette et al., 1985; Brady et al., 1981) suggest that the ATPase exists as a monomer in the membrane. However, image reconstruction studies of vanadate-induced crystals (Taylor et al., 1984), the particle distribution of freeze-fracture preparations (Napolitano et al., 1983), and target size inactivation studies (Hymel et al., 1984) have provided evidence for a dimeric functional unit. Other physical studies, such as rotary shadowing electron microscopy (Franzini-Armstrong & Ferguson, 1985) and fluorescence energy transfer (Vanderkooi et al., 1977; Fagan & Dewey, 1986), have provided evidence for the presence of higher order oligomers such as tetramers.

Several studies have shown that the aggregation state of the Ca-ATPase is temperature dependent. The motions of spin-labeled fatty acid chains covalently attached to the ATPase suggest that the enzyme disaggregates as the temperature increases (Andersen et al., 1981). This conclusion was also supported by resonance energy transfer between fluorescent fatty acids and the ATPase (Fagan & Dewey, 1986). The temperature dependence of the rotational motion of eosin-labeled SR-ATPase, determined from transient absorption anisotropy experiments, showed changes in slope that were interpreted as changes in oligomeric state (Hoffmann et al., 1979). Other studies have also reported nonlinear temperature dependence of absorption and emission anisotropy of triplet probes (Burkli & Cherry, 1981; Speirs et al., 1983). In some cases, the apparent transition temperatures occurred between 15 and 20 °C, correlating with the slope change in the Arrhenius plot of Ca-ATPase activity (Inesi et al., 1973, 1976; Bigelow et al., 1986). A similar break in the Arrhenius plot of the detergent-solubilized Ca-ATPase has been reported (Dean & Tanford, 1978), suggesting that this discontinuity is primarily due to a conformational change in the ATPase protein and not due to changes in the lipid phase. This is supported by electron paramagnetic resonance (EPR) spectra of stearic acid spin labels, which show no abrupt temperature-dependent change in the fluidity of SR lipids (Bigelow et al., 1986). Saturation transfer EPR (ST-EPR) studies of the rotational dynamics of the Ca-ATPase have correlated Ca-ATPase activity with protein rotational mobility, as perturbed by changes in lipid fluidity or protein–protein interactions (Thomas & Hidalgo, 1978; Bigelow & Thomas, 1987; Squier & Thomas, 1988; Squier et al., 1988a). ST-EPR did not reveal any discontinuity in the temperature dependence of average protein mobility (Squier et al., 1988b). The lack of time resolution in the ST-EPR studies has precluded quantitative analysis of the possible heterogeneity of protein motions and protein–protein interactions.

In the present study, we have used time-resolved phosphorescence anisotropy to probe the rotational motions of the Ca-ATPase in SR, as perturbed by changes in solvent and temperature. We have obtained higher time resolution than in most previous studies, and we have fit the anisotropy decays with fewer model-dependent assumptions. We have performed control experiments, varying the concentration of agents designed to perturb the viscosity of either the membrane or the aqueous phase, and obtaining an empirically accurate measure of the lipid viscosity, in order to assign the detected correlation times to specific protein motions. The results shed new light on the role of protein dynamics and protein–protein interactions in the Ca-ATPase reaction mechanism.

Materials and Methods

Reagents. Erythrosin 5-isothiocyanate (ERITC) was obtained from Molecular Probes Inc. (Eugene, OR) and was stored in DMF at −70 °C. Eosin-Y was obtained from Kodak. Glucose oxidase type IX, catalase, glucose, ATP, and dimyristoylphosphatidylcholine (DMPC) were obtained from Sigma. Spectral-grade glycerol was obtained from Aldrich. Fatty acid spin labels (*N*-oxyl-4′,4′-dimethyloxazolidine derivatives of stearic acid with the nitroxide at the 5- and 12-position, designated 5- and 12-SASL) were obtained from Aldrich, dissolved in DMF, and stored in liquid nitrogen.

Membrane Preparation. Sarcoplasmic reticulum (SR) vesicles were prepared from rabbit skeletal white muscle and partially purified on a discontinuous sucrose gradient, as described previously (Birmachu et al., 1989). The SR vesicles were suspended in 0.3 M sucrose, 30 mM MOPS, pH 7.0 (SR buffer), and stored in liquid nitrogen. Unless otherwise indicated, all subsequent experiments were performed in SR buffer.

Assays. Ca-dependent ATPase activity was measured in a solution containing 5 mM ATP, 0.05 mg of protein/mL, 60 mM KCl, 6 mM $MgCl_2$, 0.1 mM $CaCl_2$, 2 μM of the ionophore A23187, and 30 mM MOPS (pH 7.0), essentially as described previously (Lewis & Thomas, 1986). Protein concentrations were determined by the biuret method using bovine serum albumin (BSA) as a standard (Lewis & Thomas, 1986).

SDS Polyacrylamide Gel Electrophoresis. Sodium dodecyl sulfate– (SDS–) polyacrylamide gel electrophoresis was performed according to the method of Laemmli (1970) using 6–18% gradient slab gels with a 3% stacking gel. SR samples were diluted 1:1 with a solution containing 10 mM Tris-HCl, pH 8.0, 1% β-mercaptoethanol, 10% glycerol, and 0.05% bromphenol blue prior to loading onto the gradient gels. Bromphenol blue was omitted from samples containing protein labeled with ERITC, since the dye quenches the fluorescence of the labeled bands on the gel. Fluorescent photographs of erythrosin-labeled bands were taken through a 550-nm cutoff filter using a UV lamp, prior to staining the gels with Coomassie blue. The stained gels and the fluorescence negatives were scanned with a densitometer to quantitate the amount of protein and erythrosin, respectively.

Labeling the Ca-ATPase with ERITC. SR vesicles were labeled with erythrosin 5-isothiocyanate (ERITC) in a medium containing 30 mM Tris (pH 8.7), 5 mM $MgCl_2$, and 100 mM KCl, at a protein concentration of 3–4 mg/mL. Samples were incubated with ERITC for 45 min at 25 °C. At the end of the reaction time, the samples were diluted 5-fold with 30 mM MOPS buffer (pH 7.0), containing 5 mM $MgCl_2$, 100 mM KCl, 1 mg/mL BSA (medium A), or 0.3 M sucrose and 1 mg/mL BSA (medium B), and incubated for 20 min at 4 °C prior to centrifugation at 62000*g* for 25 min. The inclusion of BSA ensured the removal of noncovalently bound probe, as determined by absorbance of the supernatant. The pellets were washed once more in medium B and resuspended in the

same buffer. Labeled samples were kept on ice and used the same day for spectroscopic measurements. The stoichiometry of labeling was determined in the presence of 2% deoxycholate, using an extinction coefficient of 80 000 M^{-1} [determined as described by Birmachu et al. (1989)] at 536 nm and assuming a molecular weight of 115 kDa for the Ca-ATPase. The Ca-ATPase accounted for 75% of the total protein, as determined from scans of the Coomassie-stained SDS polyacrylamide gels.

Time-Resolved Phosphorescence Instrumentation. The spectrometer used to obtain phosphorescence intensity decays and anisotropy decays was described previously in detail (Ludescher & Thomas, 1988). The phosphorescence anisotropy decay $r(t)$ is given by

$$r(t) = \frac{I(t)_{vv} - GI(t)_{vh}}{I(t)_{vv} + G2I(t)_{vh}} \quad (1)$$

where $I(t)_{vv}$ and $I(t)_{vh}$ are the time-dependent decays of the phosphorescence intensities observed through polarizers oriented parallel and perpendicular to the vertically polarized excitation pulse. G is an instrumental correction factor. Intensity decays were collected for 2000 laser shots alternating in the vertical and horizontal direction for 30 loops.

Sample Preparation. Oxygen was removed from the phosphorescent samples enzymatically according to the method of Eads et al. (1984) by adding 100 μg/mL glucose oxidase, 15 μg/mL catalase, and 5 mg/mL glucose. Deoxygenation was carried out for 10–15 min prior to data collection, in sealed cuvettes (0.3 × 1.0 cm) containing 0.2–0.5 mg/mL SR protein. The samples were equilibrated at the desired temperature (±0.2 °C) for a total of 10–15 min prior to measuring phosphorescence. Diethyl ether was added to SR (0.35 mg/mL protein) in a fluorescence cuvette by injecting an aliquot of diethyl ether under the surface of the buffer. The cuvette was capped, mixed rapidly by inversion, and allowed to equilibrate for 10–15 min prior to acquiring phosphorescence decays. For experiments in aqueous glycerol solutions, the desired concentration of glycerol (w/w) was made up in 30 mM MOPS, 5 mM $MgCl_2$, 100 mM KCl, pH 7.0.

Data Analysis. The phosphorescence intensity and anisotropy decays were analyzed by a nonlinear least-squares fit to a sum of exponentials. Intensity decays were fit to a sum of exponentials:

$$I(t)/I(0) = \sum_{i=1}^{n} a_i \exp(-t/\tau_i) \quad (2)$$

where τ_i are the fluorescence lifetimes and a_i are the amplitudes. The time dependence of the phosphorescence anisotropy is described by

$$r(t)/r_0 = \sum_{i=1}^{n} A_i \exp(-t/\phi_i) + A_\infty \quad (3)$$

ϕ_i are rotational correlation times, A_i are the normalized amplitudes (r_i/r_0). A_∞ (r_∞/r_0) is the normalized residual anisotropy, and r_0 is the initial anisotropy ($r_0 = \sum r_i + r_\infty$). The number of exponentials (n in eq 2 or 3) was increased until no further improvement was observed in the fit, as evaluated from the modified χ^2 value (minimized in the least-squares fit) and the residual plot (data minus fit).

In a model-independent calculation, $r_\infty/r_0 = S^2$, where S is the order parameter of the probe's transition moment relative to the membrane normal, as affected by rotational motions in the observed time window (Lipari & Szabo, 1980). The rotational motion of membrane proteins is usually described by one of two models: (a) uniaxial rotation and (b) wobble in a cone [Cherry, 1978; Kawato & Kinosita, 1981; Kinosita et al., 1984; reviewed by Thomas (1986)]. In the uniaxial model, the protein rotates about an axis normal to the bilayer with a diffusion coefficient D_m, and the anisotropy decay is given by

$$r(t)/r_0 = A_\alpha \exp(-4D_m t) + A_\beta \exp(-D_m t) + A_\infty \quad (4)$$

A_∞ describes the extent to which the probe's motion is restricted in angular amplitude, due to the fixed angle θ_m between the probe's emission transition moment and the normal to the membrane bilayer:

$$A_\infty = \tfrac{1}{4}(3\cos^2\theta_m - 1)^2 \quad (5)$$

Equation 4 implies that each independently rotating species should give rise to two correlation times $\phi_\alpha = 1/(4D_m)$ and $\phi_\beta = 1/(D_m)$. The ratio of the two decay amplitudes is given by

$$A_\alpha/A_\beta = \tfrac{1}{4}\tan^{-2}\theta_m \quad (6)$$

In the alternative model, the whole protein or a segment of the protein undergoes restricted motion (wobbles) within the walls of a cone with a half angle θ_c and a diffusion coefficient D_w. In this case

$$r(t)/r_0 = A\exp(-tD_w/\sigma) + A_\infty \quad (7)$$

where $A_\infty = [0.5\cos\theta_c(1 + \cos\theta_c)]^2$, and σ is a function of θ_c (Lipari & Szabo, 1980).

EPR Measurements of Lipid Viscosity and Effective Protein Radius. The rotational diffusion coefficient (D_m in eq 4) for uniaxial rotation of a cylindrical membrane protein can be expressed as a function of the membrane lipid viscosity (η), temperature (T), and the effective radius (a) of the portion of the protein in the bilayer (Saffman & Delbrück, 1975):

$$D_m = kT/(4\pi a^2 h\eta) \quad (8)$$

where h is the thickness of the lipid bilayer (assumed to be 45 Å). Therefore, the effective radius a of the Ca-ATPase can be determined from the phosphorescence data if the lipid viscosity η is known.

The viscosity of SR lipid has been measured over a wide range of temperatures, using the EPR spectra of stearic acid spin labels in SR lipid, calibrated by experiments in reference solvents (Squier et al., 1988b). This method produces a viscosity value that is proportional to the protein rotational correlation time, as predicted by eq 8, but dependent on the depth of the spin label in the lipid bilayer (Squier et al., 1988b). While this is physically realistic, reflecting the fludity gradient of the bilayer (Hubbell & McConnell, 1971; Squier & Thomas, 1989), in the present study we require a depth-independent viscosity that allows us to use eq 8 to calculate accurately the effective radius a. Therefore, we must calibrate our spin-label assay empirically, by performing it on a model system for which the depth-independent viscosity (as defined by eq 8) is accurately known. The intramembrane radius of bacteriorhodopsin [a = 17.5 Å (Hendersen & Unwin, 1975)] and its rotational diffusion coefficients in dimyristoylphosphatidylcholine (DMPC) membranes at 25 °C [$\phi_m = 1/D_m$ = 15.6 μs (Cherry & Godfrey, 1981)] have been determined, allowing us to solve eq 8 for the viscosity of DMPC at 25 °C: η = 3.7 P. The next step is to perform the spin-label assay of Squier et al. (1988b) on the same DMPC system and to compare the apparent viscosity (determined from EPR) with the actual viscosity (3.7 P).

Multilamellar dispersions of DMPC, prepared by vortexing, were labeled with fatty acid spin labels 5-SASL and 12-SASL, essentially as described by Squier et al. (1988b). The spin label (either 5-SASL or 12-SASL), dissolved in DMF, was added

Table I: Phosphorescence Intensity Decay Parameters of ERITC-SR at 4 °C[a]

τ_1 (μs)	τ_2 (μs)	τ_3 (μs)	τ_4 (μs)	a_1	a_2	a_3	a_4	χ^2
300				1.0				86.3
(38)								
80	380			0.10	0.90			4.4
(3)	(5)			(0.02)	(0.02)			
8	107	384		0.05	0.09	0.87		2.5
(1)	(3)	(10)		(0.02)	(0.02)	(0.02)		
7	86	325	412	0.05	0.07	0.32	0.56	2.5
(1)	(3)	(9)	(4)	(0.02)	(0.02)	(0.02)	(0.02)	

[a] Phosphorescence lifetimes τ_i were obtained from a nonlinear least-squares fit of the total (unpolarized) phosphorescence intensity decays of ERITC attached to the Ca-ATPase in rabbit skeletal SR, at 4 °C, at 0.3 mg of protein/mL in 30 mM MOPS, 0.3 M sucrose, pH 7.0. SR vesicles were labeled with ERITC at 0.8 ± 0.1 mol of ERITC bound per ATPase. The data were fit according to a sum of exponentials, with n varying from 1 to 4 (eq 1). τ_1, τ_2, τ_3, and τ_4 are the triplet excited state lifetimes with fractional contributions a_1, a_2, a_3, and a_4, respectively. χ^2 values are representative of the individual measurements. The values are averages of four experiments on two labeled preparations. Values in parentheses are the standard errors of the mean.

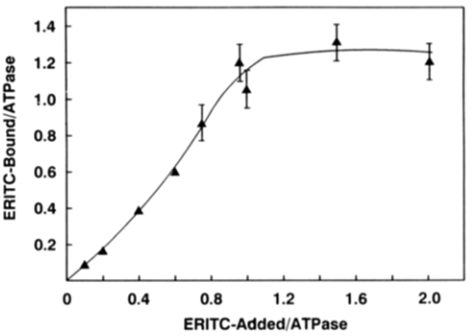

FIGURE 1: Binding of ERITC to SR. Samples containing 2–3 mg/mL of SR in 5 mM $MgCl_2$, 0.1 M KCl, 30 mM Tris (pH 8.7) were covalently modified with ERITC at the designated ERITC/ATPase (mole/mole) ratio.

to a 30 mM DMPC dispersion in SR buffer at a ratio of 200 phospholipids per spin label and incubated for 5 min at 35 °C with intermittent vortexing. Conventional EPR spectra were recorded at 25 °C, following the procedure described by Squier et al. (1988b), and the order parameters were measured by using eq 2 of Squier et al. (1988b), using values of T_0 (the isotropic hyperfine coupling constant) = 14.3 and $T_\perp$ (the minimum hyperfine coupling constant) = 6.3 G (Squier & Thomas, 1989). The lipid viscosity η (inverse of fluidity) was then determined by use of the calibration curve in Figure 2 of Squier et al. (1988b).

Results

Specificity of Labeling. The binding of ERITC to the Ca-ATPase saturates at 1.15 ± 0.15 mol of ERITC bound per mole of ATPase (Figure 1). SR vesicles for phosphorescence anisotropy experiments were routinely labeled at 0.9 mol of ERITC added per ATPase, giving 0.8 ± 0.1 mol of ERITC bound per ATPase. Inhibition of Ca-ATPase activity parallels covalent labeling with ERITC, with complete inhibition of activity occurring at 1.05 ± 0.15 mol of ERITC bound per mole of ATPase (data not shown). This is consistent with the inhibition of ATPase activity by other isothiocyanate derivatives, such as FITC, which reacts specifically with lysine 515 near the ATP binding site (Mitchinson et al., 1982; MacLennan et al., 1985). Densitomer scans of the fluorescent and Coomassie blue stained gels of ERITC-SR, with 0.85 ± 0.12 ERITC bound per ATPase (Figure 2), showed that 90 ± 5% of the fluorescence intensity is associated with the 115-kDa ATPase band. The high specificity of labeling is comparable to that obtained for labeling SR with fluorescein 5-isothiocyanate (FITC) (Birmachu et al., 1989) and is in agreement with the specificity reported previously for the modification

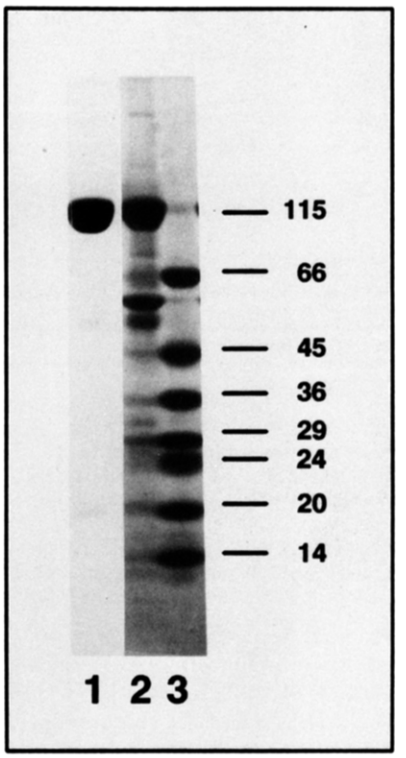

FIGURE 2: SDS gel electrophoresis of ERITC-SR. Samples were run on 6–18% gradient polyacrylamide gels. Photographs of (1) the fluorescent gel (negative image), (2) the Coommassie blue stained gel, and (3) molecular weight standards are shown. Molecular weight standards are bovine albumin (66 kDa), ovalbumin (45 kDa), glyceraldehyde 3-phosphate dehydrogenase (36 kDa), carbonic anhydrase (29 kDa), trypsinogen (24 kDa), trypsin inhibitor (20.1 kDa), and α-lactalbumin (14.2 kDa). The position of the Ca-ATPase at 115 kDa is also marked.

of the Ca-ATPase with FITC (Mitchinson et al., 1982).

Phosphorescence Emission Decay. The decay of the total (unpolarized) phosphorescence emission intensity of ERITC-SR at 4 °C was best fit by a three-exponential function (n = 3 in eq 2). No significant improvement was obtained by increasing n to 4, as judged by the χ^2 values (Table I) and the residual plots (not shown). The predominance (87 ± 2%) of one lifetime (τ_3 = 384 ns) in the three-exponential fit supports the high specificity of labeling (90 ± 5%) determined from gel electrophoresis. Therefore, the saturation of labeling (Figure 1), gel electrophoresis (Figure 2), and phosphorescence emission decay (Table I), taken together, strongly indicate that at least 85% of the label is attached to a single site on the Ca-ATPase.

Table II: Phosphorescence Anisotropy Decay Parameters for ERITC-SR at 4 °C[a]

ϕ_1 (μs)	ϕ_2 (μs)	ϕ_3 (μs)	ϕ_4 (μs)	A_1	A_2	A_3	A_4	r_0	A_∞
180				0.0669					
(16)				(0.0059)					
29	258			0.231	0.523			0.113	0.248
(3)	(9)			(0.010)	(0.012)			(0.003)	(0.022)
13	77	314		0.114	0.137	0.430		0.114	0.227
(3)	(11)	(23)	(0.004)	(0.014)	(0.023)			(0.005)	(0.022)
7	43	188	554	0.107	0.140	0.311	0.264	0.117	0.179
(3)	(3)	(51)	(192)	(0.020)	(0.056)	(0.041)	(0.038)	(0.004)	(0.048)

[a] Phosphorescence anisotropy parameters obtained from a nonlinear least squares analysis (eq 3) of phosphorescence anisotropy decays of ERITC-SR. Experimental conditions were as outlined in Figure 3. ϕ_1, ϕ_2, ϕ_3, and ϕ_4 are the rotational correlation times, and A_1, A_2, A_3, and A_4 are the amplitudes normalized to r_0. r_0 is the fit value of the anisotropy extrapolated to zero time, and $A_\infty = r_\infty/r_0$ is the normalized residual anisotropy. The values are averages of 10 experiments on five labeled preparations. Values in parentheses are the standard errors of the mean. The χ^2 values listed in the legend to Figure 3 for the one-, two-, three-, and four-exponential fits are representative for the data shown in this table.

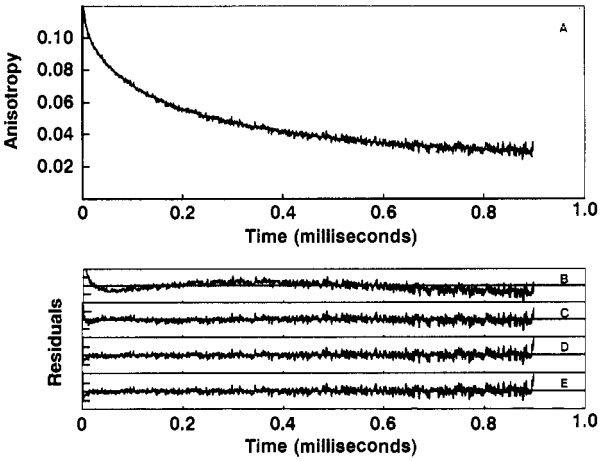

FIGURE 3: Phosphorescence anisotropy decay of the ERITC-labeled Ca-ATPase in rabbit skeletal SR, in 30 mM MOPS buffer containing 0.3 M sucrose at 4.0 ± 0.3 °C. A: data superimposed on the fit to a sum of three exponentials plus a constant (eq 3). B–E are the residuals for the fit to one-, two-, three-, and four-exponential functions, respectively. The corresponding χ^2 values are 28.2, 6.6, 5.6, and 5.8, respectively. Experimental conditions were as described in the legend to Table I.

Phosphorescence Anisotropy Decay. The phosphorescence anisotropy decays of ERITC-SR at 4 °C were fit to eq 3, varying n to obtain the best fit (Figure 3, Table II). The nonrandom residual plots for n = 1 and 2 (Figure 3, B and C), along with the high χ^2 values (28.22 and 6.68, Table II), clearly indicate that the decay is not adequately fit by a sum of one or two exponentials plus a constant. Both the χ^2 value (5.6) and residual plot (Figure 3D) are improved by increasing n to 3, but no improvement is obtained by increasing n to 4 (χ^2 = 5.8, Figure 3E), indicating that a four-exponential fit is not justified. These results were consistently found under all the conditions of this study. Therefore, further analysis will consider only the fit to three exponentials plus a constant (n = 3 in eq 3).

The three-exponential fit of the phosphorescence anisotropy decay at 4 °C gave rotational correlation times ϕ_1 = 13 ± 3 μs, ϕ_2 = 77 ± 11 μs, and ϕ_3 = 314 ± 23 μs (Table II). The amplitudes corresponding to the three correlation times were A_1 = 0.114 ± 0.004, A_2 = 0.137 ± 0.014, and A_3 = 0.430 ± 0.023. We tested the effect of 0.3 M sucrose (approximately 10% sucrose w/v) on the phosphorescence anisotropy decay and found no significant difference in the presence and absence of this low concentration of sucrose. We also tested the possibility that resonance energy transfer between ERITC molecules may affect the phosphorescence anisotropy decay. We found that the level of modification of the ATPase with ERITC had no effect on the phosphorescence anisotropy decay, with preparations labeled at 0.3 and 0.9 mol of ERITC bound per mole of ATPase giving essentially identical decays, indicating that energy transfer can be ruled out as a mechanism of phosphorescence depolarization in our ERITC-SR preparations.

Effects of Solution Viscosity. In order to assign the rotational correlation times to the rotational mode(s) of the ATPase, we first performed experiments to rule out a contribution of vesicle rotation to the phosphorescence anisotropy. The size distribution of the SR vesicle preparation is heterogeneous. The average radius is 700 ± 170 Å, and 10–25% of the vesicles have radii in the 500–600-Å range (Lewis & Thomas, 1986; Thomas & Hidalgo, 1978). According to the Stokes–Einstein equation ($\phi_v = 4\pi r^3\eta/3kT$, where k is Boltzmann's constant and η is viscosity), the rotational correlation time ϕ_v predicted for a sphere with a radius of 600 Å at 4 °C in water (viscosity 1.62 cP) is approximately 400 μs, which is not much greater than ϕ_3 (314 = ±23 μs). Thus, a small but significant fraction of the vesicles could contribute to the anisotropy decay in the time window 0–1 ms. Although Stokes–Einstein equation has not been quantitatively validated for membrane vesicles, this possibility must be tested. Therefore, we modulated the viscosity of the bulk aqueous medium (using glycerol).

We measured the phosphorescence anisotropy of ERITC-SR in the presence of varying concentrations of glycerol (0–67% w/w glycerol) at 25 °C. Glycerol increases the viscosity of the aqueous solution (by a factor of 10 at 64% glycerol) but does not have a significant effect on the membrane viscosity, as measured from the lipid hydrocarbon mobility (Squier & Thomas, 1988). ϕ_1 and ϕ_2 are essentially independent of solution viscosity (Figure 4), indicating that these two correlation times correspond to protein rotation within the membrane, not to vesicle tumbling. ϕ_3 increases slightly as the solution viscosity increases from 0.010 to 0.025 P (30% glycerol), but remains essentially constant above this value. The dependence of ϕ_3 on solution viscosity is much less than predicted for vesicles of radius r = 500 and 600 Å, calculated from the Stokes–Einstein equation for the rotation of a spherical particle (see Figure 4), indicating that ϕ_3 is not determined by vesicle rotation. However, we cannot unequivocally rule out some contribution from vesicle rotation based on the data in Figure 4 alone.

The dependence of the phosphorescence anisotropy amplitudes provides us with additional information on this point (Figure 5). First, A_∞ (the normalized residual anisotropy) does not depend much on solution viscosity. If the observed independence of ϕ_3 at high viscosity is due to vesicles that have been slowed down by increasing solvent viscosity, so as to move them out of the time window of observation, this should be reflected in a significant increase in A_∞, which is not observed.

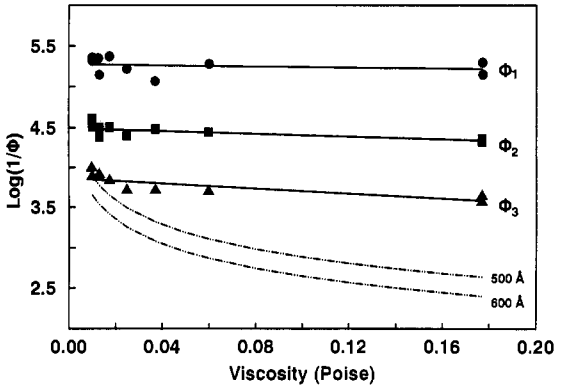

FIGURE 4: Effect of glycerol on the rotational correlation times of ERITC-SR at 25 °C. Glycerol/buffer mixtures (w/w) were made in 30 mM MOPS, 100 mM KCl, 5 mM $MgCl_2$, pH 7.0. Solid lines are the best fit lines drawn through the viscosity dependence of the rotational correlation times ϕ_1 (circles), ϕ_2 (squares), and ϕ_3 (triangles). Dashed lines show the viscosity dependence predicted for vesicles with radii of 500 and 600 Å, according to the Stokes–Einstein equation ($\phi = 4\pi r^3\eta/3kT$, where k is Boltzman's constant and η is viscosity).

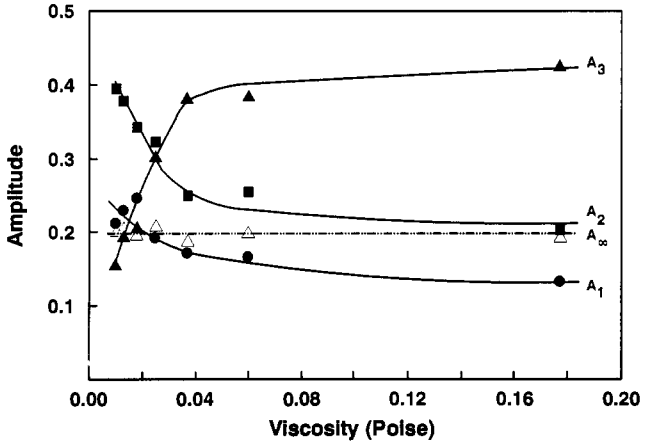

FIGURE 5: Effect of glycerol on the phosphorescence anisotropy amplitudes A_1 (circles), A_2 (squares), A_3 (solid triangles), and A_∞ (open triangles) of ERITC-SR at 25 °C. Experimental conditions were as described in Figure 4.

Second, there is a decrease in A_1 and A_2 and a reciprocal increase in A_3 (Figure 5), suggesting that the components corresponding to ϕ_1 and ϕ_2 are being converted to the slower (probably larger, more aggregated) component corresponding to ϕ_3. Since glycerol has been reported to result in the dehydration and subsequent aggregation of the Ca-ATPase within the membrane (Van Winkle et al., 1985; Squier & Thomas, 1988; Taylor et al., 1988), it is likely that the anisotropy changes reflect this aggregation. Although Figures 4 and 5, taken together, provide strong evidence that vesicle rotation does not contribute significantly to the phosphorescence anisotropy decay, we investigated the dependence of the anisotropy decay on lipid viscosity to test this conclusion further.

Effects of Lipid Viscosity. Diethyl ether partitions preferentially into the SR membrane and activates both ATPase activity and Ca transport (Salama & Scarpa, 1983). At the highest concentration of ether used in the present study (6% v/v), the aqueous ether concentration is only 0.2 mM, which has virtually no effect on the viscosity of the aqueous solution. The addition of diethyl ether to SR vesicles has been shown to decrease the viscosity (increase the fluidity) of the lipid phase of the membrane, as determined by EPR spectroscopy using fatty acid spin labels. The effect of the addition of 6% (v/v) diethyl ether on lipid viscosity in SR is equivalent to increasing the temperature by approximately 10 °C, resulting in a decrease in membrane viscosity by a factor of 2 (Bigelow

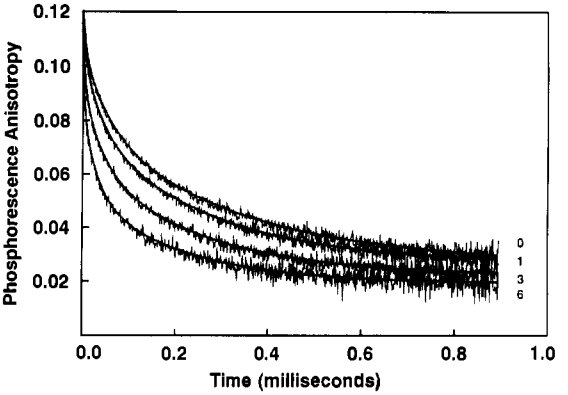

FIGURE 6: Effect of diethyl ether on the phosphorescence anisotropy of ERITC-SR at 4.0 °C. Ether was added to 0.35 mg of SR protein/mL in 30 mM MOPS, 0.3 M sucrose, as described in Materials and Methods. The phosphorescence decays shown are for 0, 1, 3, and 6% diethyl ether (v/v).

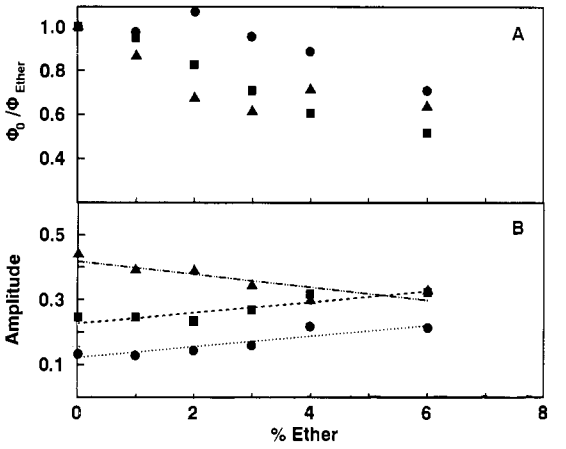

FIGURE 7: Effect of diethyl ether on the phosphorescence anisotropy parameters of ERITC-labeled SR at 4.0 °C. Parameters were obtained from a least-squares fit to a function of the sum of three exponentials plus a constant. Panel A: effect of ether on correlation times ϕ_1 (circles), ϕ_2 (squares), and ϕ_3 (triangles). Panel B: effect of ether on amplitudes A_1 (circles), A_2 (squares), and A_3 (triangles).

& Thomas, 1987). The phosphorescence anisotropy decay of ERITC-SR becomes progressively more rapid in the presence of diethyl ether at 4 °C, without a significant change in the residual anisotropy (Figure 6). All three correlation times decrease with increasing ether (Figure 7A), indicating that they originate in protein motion limited by lipid viscosity. The decrease in correlation times at 6% ether is comparable to the 50% decrease in lipid viscosity (Bigelow & Thomas, 1987), which should limit protein rotational motion within the membrane (Saffman & Delbrück, 1975), but is much greater than the change in aqueous viscosity, which should limit vesicle rotation only. If ϕ_3 originated from vesicle rotation but ϕ_2 (which is clearly independent of vesicle rotation, as shown in Figure 4) originated from protein rotation within the membrane, ϕ_2 would depend more than ϕ_3 on membrane viscosity. The amplitudes also vary with concentration of ether (Figure 7B), with A_1 and A_2 increasing and A_3 decreasing, again suggesting that there is interconversion of rotational species, with ether increasing the fraction of the more mobile components. As in the case of glycerol effects (Figure 5), these substantial changes in correlation times and amplitudes are accompanied by an essentially constant A_∞ (0.196 ± 0.008, data not shown), which is most consistent with rotation of the protein about the membrane normal, as discussed further below. Therefore, the dependence of the rotational correlation times and amplitudes on the solution viscosity (Figures 4 and

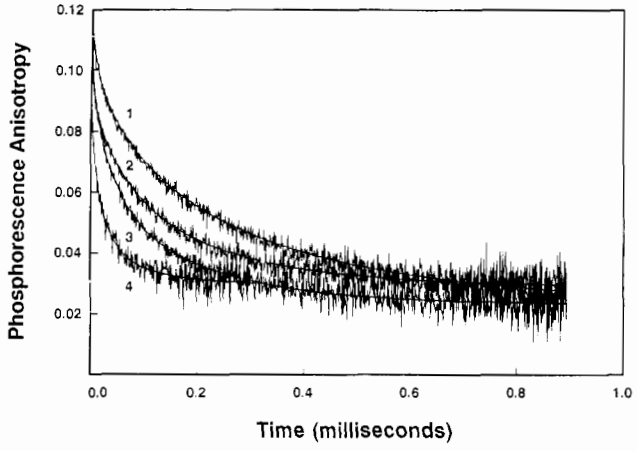

FIGURE 8: Dependence of the phosphorescence anisotropy of ER-ITC-SR on temperature. The decays shown are for (1) 3.5 °C, (2) 7.7 °C, (3) 10.7 °C, and (4) 26.7 °C.

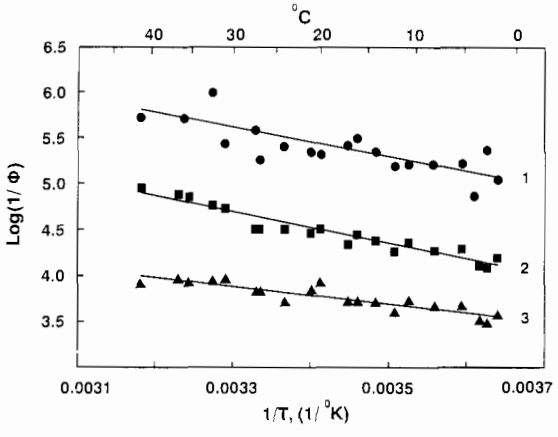

FIGURE 9: Arrhenius plot of the rates of protein rotation (1) $1/\phi_1$, (2) $1/\phi_2$, and (3) $1/\phi_3$. Linear regression coefficients for ϕ_3, ϕ_2, and ϕ_1 were 0.82, 0.92, and 0.54.

5) and on the membrane lipid viscosity (Figures 6 and 7), taken together, provides strong evidence that the phosphorescence anisotropy decay of ERITC-SR reflects protein motion within the membrane, limited by membrane lipid viscosity and protein association, and does not reflect the rotation of membrane vesicles.

Effects of Temperature. In order to characterize further the rotational motions of the Ca-ATPase, we recorded phosphorescence anisotropy decays of ERITC-SR from 2 to 41 °C (Figure 8). All three correlation times decreased with temperature. The Arrhenius plots for the rates of protein motion ($1/\phi_1$, $1/\phi_2$ and $1/\phi_3$) are essentially linear (Figure 9). The activation energies calculated for $1/\phi_1$, $1/\phi_2$, and $1/\phi_3$ were 7.4 ± 1.6, 7.9 ± 0.4, and 4.4 ± 0.7 kcal/mol, respectively.

The amplitudes also vary with temperature (Figure 10). A_3 is the major component (0.43) at 4 °C but decreases to 0.15 at 20 °C. There is a concomitant increase in A_2 from 0.14 at 4 °C to 0.40 at 20 °C, suggesting the conversion of one species (corresponding to ϕ_3) to another (more mobile, corresponding to ϕ_2) over this temperature range. Above 20 °C, A_3 remains constant and small at 0.15, while A_2 decreases slightly and A_1 continues to increase and becomes the major component at 40 °C. In contrast, both r_0 (0.111 ± 0.006) and A_∞ (0.215 ± 0.012) remain essentially constant (data not shown).

Since variations in membrane fluidity induced by either ether (Figure 7) or temperature (Figure 10) suggest that the amplitudes are proportional to the mole fractions of interconverting species, we made a van't Hoff plot of the apparent

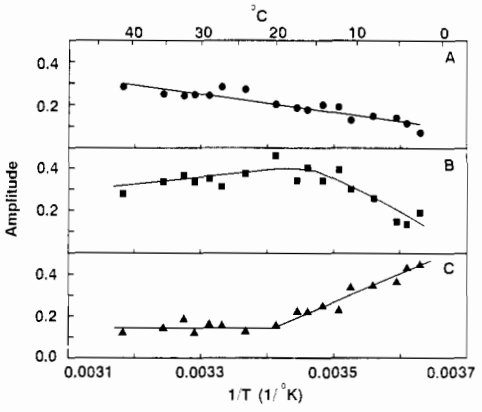

FIGURE 10: Effect of temperature on the phosphorescence anisotropy amplitudes. Panel A, A_1; panel B, A_2; and panel C, A_3.

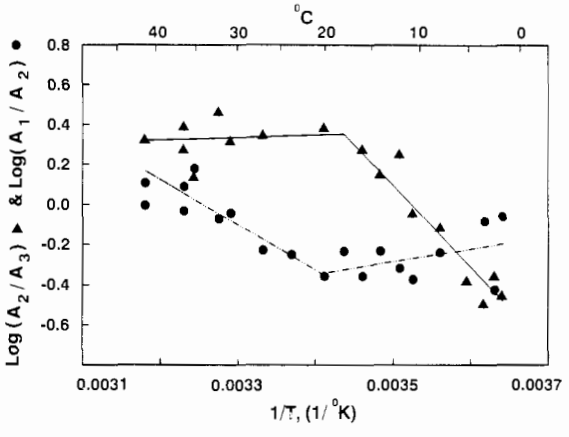

FIGURE 11: Temperature dependence of the apparent equilibrium constants calculated from the amplitudes A_1, A_2, and A_3. The regression line for A_2/A_3 below 20 °C (R = 0.93) gave values for enthalpy and entropy changes of 19 ± 2 kcal mol^{-1} deg^{-1} and 66 ± 1 cal mol^{-1} deg^{-1}, respectively.

equilibrium constants A_2/A_3 and A_1/A_2 (Figure 11). Distinct changes in the slopes are evident in the range of 18–23 °C. The apparent enthalpy change calculated for A_2/A_3 below 20 °C was 19 ± 2 kcal mol^{-1} deg^{-1}, with an entropy change of 66 ± 1 cal mol^{-1} deg^{-1}.

Measurement of Membrane Lipid Viscosity. EPR measurements on DMPC gave order parameters of 0.60 ± 0.02 and 0.30 ± 0.02 for 5-SASL and 12-SASL, respectively, corresponding to effective viscosity values of 3.7 ± 0.2 and 0.7 ± 0.1 P, using the method of Squier et al. (1988b). This reflects the well-established fluidity gradient in the bilayer (Hubbell & McConnell, 1971). The viscosity determined with 5-SASL is in excellent agreement with the known viscosity η of DMPC (3.7 P), as determined empirically from the known diffusion coefficient D_m and radius a of bacteriorhodopsin, using eq 8 (see Materials and Methods). Therefore, the viscosity η of the SR membrane, needed for the calculation of the protein's radius a (from the diffusion coefficient D_m, using eq 8), was determined from EPR spectra of 5-SASL in SR lipids (Squier et al., 1988b). The results are summarized in Table III and discussed below.

Discussion

Summary of Results. We have found the rotational motion of the ATPase to be complex and heterogeneous. It is only because of the time resolution of our method, coupled with systematic variation of temperature, bulk viscosity, and lipid viscosity, that we have been able to evaluate these complex motions with some rigor. We have gone beyond previous studies of Ca-ATPase motion, in an attempt to evaluate

Table III: Lipid Viscosity and Effective Protein Radii[a]

temp (°C)	S	η (P)	ϕ_1 (μs)	a_1 (Å)	ϕ_2 (μs)	a_2 (Å)	ϕ_3 (μs)	a_3 (Å)
4	0.75 ± 0.03	7.7 ± 0.5	13 ± 3	22 ± 8	77 ± 11	52 ± 10	314 ± 23	106 ± 8
20	0.53 ± 0.03	2.6 ± 0.3	5 ± 1	24 ± 4	35 ± 4	64 ± 6	186 ± 35	148 ± 22

[a] S, order parameter for 5-SASL in SR lipids [Squier et al. (1988b), Figure 4]. η, viscosity calculated from S [Squier et al. (1988b), Figure 5]. a_i, effective radius of a cylindrical protein corresponding to ϕ_i and η, calculated from eq 8 and eq 4, with h = 45 Å. The a_i values shown correspond to $\phi_i = 1/(4D_{mi})$, which amounts to assuming that $A_\alpha \gg A_\beta$ in eq 4. If $A_\beta \gg A_\alpha$, then the estimated a_1 values are exactly half those shown above. As discussed in the text, both sets of radii are possible, but the larger (α) set is most consistent with the data and the known dimensions of Ca-ATPase oligomers.

quantitatively the contributions of methodological artifacts and evaluate the functional significance of the rotational dynamics of the ATPase.

Labeling Specificity. Since less than 15% of the probes are attached to sites other than the Ca-ATPase active site (as shown in Results), it is unlikely that the small contribution of this minor fraction to the phosphorescence anisotropy decay is great enough to affect the conclusions of this study. Even if 15% of the probes are attached to another site, the normalized amplitude (A in eq 3) of this component would be no greater than 0.12, which is less than the values observed for the three amplitudes A_i under most conditions (Figures 5, 7, and 10).

Viscosity Effects. The independence of ϕ_1 and ϕ_2 and the weak dependence of ϕ_3 on aqueous viscosity (Figure 4), combined with the changes in amplitudes (Figure 5), indicate that vesicle rotation, which should have a correlation time proportional to the aqueous viscosity (eq 8, Figure 4), is not responsible for the anisotropy decay. The conclusion that vesicle tumbling does not contribute significantly to the microsecond rotational motion of the Ca-ATPase in SR is consistent with previous ST-EPR studies of spin-labeled SR (Thomas & Hidalgo, 1978; Squier et al., 1988a). The correlation times do decrease as the lipid viscosity decreases (Figure 7), as expected if the anisotropy decay reflects the rotation of the protein within the membrane. This is consistent with previous EPR studies of lipid viscosity and protein rotation in SR, as modulated by ether (Bigelow & Thomas, 1987), lipid substitution (Thomas & Hidalgo, 1978; Hidalgo et al., 1978), or temperature (Squier et al., 1988b). The present study indicates that changes in lipid viscosity have two types of effects—the correlation times are roughly proportional to the lipid viscosity, consistent with eq 8 (Squier et al., 1988b), while the amplitudes of the slowest decay terms increase (at the expense of the faster terms) with viscosity, consistent with previous suggestions that protein aggregation in SR (and other systems) is promoted by increases in lipid viscosity (Thomas & Hidalgo, 1978; Hidalgo et al., 1978). Glycerol has only slight effects on the correlation times, consistent with its negligible effect on SR lipid viscosity (Squier & Thomas, 1988), but it has large effects on decay amplitudes, consistent with its tendency to induce protein aggregation in SR (Van Winkle et al.,1985; Squier & Thomas, 1988; Taylor et al., 1988).

Rotational Diffusion Models. Although we have treated the anisotropy decay in an essentially model-independent manner by fitting it to a sum of exponentials and a constant, further insight can be gained by considering specific models of protein rotation to explain the decay. A key observation is that, despite large effects of glycerol, ether, and temperature on the correlation times and amplitudes, the normalized residual anisotropy (A_∞) remains essentially constat at a value of 0.20 (e.g., see Figure 5). Therefore, the order parameter, describing the amplitude of rotational motions within the observed time window, is invariant (Thomas, 1986). As mentioned above, this tends to rule out models in which some motions become too slow to measure, as predicted for vesicle tumbling at high solution viscosity, or for the formation of very large aggregates (Cherry & Godfrey, 1981): It also tends to rule out the wobble-in-cone model (eq 7), since temperature or viscosity changes would be expected to affect the amplitude of segmental protein motions (Cherry & Godfrey, 1981; Thomas, 1986). In contrast, the constant value of A_∞ is quite consistent with the uniaxial rotation model, in which there is a constant orientation of the probe with respect to the membrane normal (Cherry & Godfrey, 1981; Thomas, 1986). By use of the value of A_∞ obtained at 20 °C (0.204 ± 0.015), eq 5 gives a value of either 37 ± 2 or 80 ± 3° for θ_m, the angle between the probe's emission transition moment and the membrane normal. Thus, eq 6 gives a value of either 0.14 ± 0.03 or 7.4 ± 0.4 for the ratio of the two predicted decay terms corresponding to one rotating species. In either case, this greatly simplifies the analysis, since it implies that the decay for each rotating species should be dominated by one of the two decay terms. Given the signal-to-noise ratio (Figure 3), the minor component would be too small to detect, since its fractional amplitude A would never be larger than 0.005. *Therefore, we can analyze each decay term as a separate rotating protein species*, with each $\phi_i = 1/D_{mi}$ or $1/(4D_{mi})$ (corresponding to dominance of A_α or A_β in eq 4). It follows directly that $A_i/(\sum A_i) = A_i/0.80$ is the mole fraction of that rotating species. This provides further support for the validity of the van't Hoff plot in Figure 11.

An alternative interpretation is suggested by the relatively constant ratio A_1/A_2 (0.50 ± 0.05) as a function of glycerol (Figure 5) or ether (Figure 7). By itself, this observation suggests that these two decay terms correspond to one uniaxially rotating species (A_α and A_β in eq 4). However, this ratio yields a value of 54.7 ± 2° for θ_m (eq 6), which would require $A_\infty = 0 \pm 0.05$ (eq 5), in contradiction to the observed value $A_\infty = 0.20 \pm 0.02$. Therefore, this interpretation would be possible only if we assumed that the entire residual anisotropy was due to a separate species with no submillisecond rotational motion (or with θ_m exactly = 0°), and no temperature- or viscosity-dependent equilibration with the mobile species. This model is further discounted by the variation of A_1/A_2 with temperature (Figure 11), which is consistent with the model only if θ_m changes with temperature (but not with glycerol or ether) and the other species happen to change in a way that keeps A_∞ constant.

Effective Radii and Oligomeric States of the Rotating Species. Since we now have accurate values for the membrane viscosity η at 4 and 20 °C (Table III), and we have two possible values for each diffusion coefficient (from eq 4), we are in a good position to use eq 8 (Saffman & Delbrück, 1985) to solve for the effective radii of the labeled protein species rotating in the SR membrane. This calculation assumes that the rotating species are cylindrical, rotating only about the membrane normal, and that the only significant source of friction limiting the diffusion is that due to the surrounding lipid. These assumptions have been shown to be valid for bacteriorhodopsin (Cherry & Godfrey, 1981). The radii

calculated at 4 and 20° are in good agreement, except that the radius a_3 is significantly larger at 20° (Table III). The radius values a_i shown in Table III correspond to $\phi_i = 1/(4D_{mi})$, corresponding to $A_\alpha \gg A_\beta$ in eq 4. However, as discussed above, it is also possible that $A_\beta \gg A_\alpha$, corresponding to $\phi_i = 1/D_{mi}$ (eq 4), which would lead to radius values exactly half those shown in Table III. Without a direct measurement of the probe orientation, we cannot rigorously choose between these two sets of radii, differing by a factor of 2, but the known dimensions of Ca-ATPase monomers and oligomers offer some useful insight.

A radius of 28 Å has been reported for the monomeric form of the Ca-ATPase, determined from X-ray and neutron diffraction (Herbette et al., 1985) and from optical diffraction of freeze-fracture electron micrographs of SR (Napolitano et al., 1983). The unit cell dimensions of the vanadate-induced Ca-ATPase dimer, determined from image reconstruction of electron micrographs of crystalline membrane tubules, are 66 by 114 Å (Taylor et al., 1984), corresponding to an average radius of 57 Å. A random distribution of small aggregates (assigned to Ca-ATPase dimers and tetramers) has been observed in freeze-fracture electron micrographs of SR (Franzini-Armstrong & Ferguson, 1985). The center-to-center distance of the larger aggregates (assigned to tetramers) was 133 ± 11 Å. Thus, for the smaller of the two sets of calculated radii (half the values shown in Table III), a_1 (11–12 Å) is too small even for a monomer, while a_2 (26–32 Å) and a_3 (53–74 Å) are in good agreement with the radii of a monomer and a dimer, respectively. The small value of a_1 suggests that this component could have contributions from either smaller proteins or from segmental motion within the protein. However, neither of these interpretations for a_1 seems likely, in light of (1) the high specificity of labeling and (2) the constant value of A_∞, as discussed above. Another shortcoming of the smaller set of radii is the absence of a larger value consistent with the tetramers reported by Franzini-Armstrong and Ferguson (1985). For the larger (α) set of radii, a_1 (22–24 Å) and a_2 (52–64 Å) are in excellent agreement with the predicted radii of a monomer and a dimer, respectively, while a_3 (106–148 Å) is consistent with a tetramer or larger oligomer. Thus the larger set of radii (those shown in Table III) seems most consistent with the data and the known dimensions of Ca-ATPase oligomers. The larger temperature dependence of a_3 suggests that ϕ_3 corresponds to a distribution of aggregate sizes that changes with temperature.

Thus a strict interpretation in terms of a few specific oligomeric species is probably an oversimplification, forced upon us by the limited resolution of our detection, and the actual distribution of oligomeric species could be even more heterogeneous (Fagan & Dewey, 1986; Squier et al., 1988a). Although the detailed assignments are speculative, our general conclusions, that the observed rotational motion reflects temperature- and viscosity-dependent protein–protein association, and that these associations are heterogeneous, do not depend on specific assignments of correlation times. Regardless of these assignments, the constant value of A_∞ suggests that the relatively small aggregates contributing to the decay are not in equilibrium with a substantial population of large aggregates that are too slow to detect. This does not contradict the proposal that large-scale protein–protein associations occur (Fagan & Dewey, 1986), but they do not occur in a way that causes immobilization of a substantial fraction of Ca-ATPase molecules.

The interconversion of species suggested by the reciprocal changes in anisotropy decay amplitudes as a function of glycerol, ether, and temperature may result from (a) changes in the sizes of Ca-ATPase homooligomers, as suggested above, or (b) changes in the association of the Ca-ATPase with other proteins, for example, the 53-kDa glycoprotein that has been postulated to modulate the function of the Ca-ATPase (Kutchai & Campbell, 1989). The structure of this glycoprotein in the membrane and the degree of its association with the Ca-ATPase are not known. The sequence of the glycoproteins, recently determined from cDNA (Leberer et al., 1989), shows a highly hydrophilic protein with only two possible transmembrane segments, which are not long enough to span the membrane. Most of the protein mass is believed to reside on the luminal side of the membrane. Therefore, even if there is a tight association of the glycoprotein with the Ca-ATPase, its contribution to the cross-sectional area, and hence its effect on the rotational motion (eq 8), of the Ca-ATPase would probably not be significant unless it caused Ca-ATPase molecules to aggregate with each other.

Relationship to the Previous Anisotropy Study of ER-ITC-SR. A previous study of the rotational dynamics of the Ca-ATPase using phosphorescence anisotropy of ERITC-SR was limited to a single temperature (25 °C) and glycerol concentration (66% v/v) (Restall et al., 1984). The results obtained in that study are consistent with those obtained under comparable conditions in the present study—the anisotropy decay was best fit to a sum of three exponentials plus a constant, and the correlation times and amplitudes were similar to ours. However, the model they chose to explain their data included only a single uniaxially rotating species, assumed to be a monomer, along with a rapid wobble-in-a-cone and an immobile fraction. As discussed above, the invariance of A_∞ argues against the wobble-in-cone model. Their assumption that the slowest detected motions correspond to a monomer is also not very plausible, since it would require a viscosity of 20–25 P (Restall et al., 1984), which is at least 10 times the actual value for SR at 25 °C, determined as in Table III [1.9 ± 0.2 P (Squier et al., 1988b)].

Temperature Dependence. Arrhenius plots of the rates of protein rotation are linear (Figure 9), ruling out a sudden change in protein shape or lipid viscosity over the temperature range studied. This is consistent with previous EPR studies correlating lipid viscosity with protein rotation in SR (Bigelow et al., 1986; Squier et al., 1988b). The amplitudes of protein rotation depend in a complex manner on lipid viscosity as modulated by ether (Figure 7) and temperature (Figure 10), with apparent reciprocal changes that suggest interconversion of rotational species. The effect of 6% diethyl ether on the rotational correlation times and amplitudes was equivalent to the effect of an increase in temperature by 9 ± 2 °C, in agreement with a previous EPR study (Bigelow & Thomas, 1987). This suggests that the underlying factor for the interconversion of the rotational species is the lipid viscosity, which limits protein rotation.

The temperature dependence of anisotropy (Figures 8–11) provides insight into a long-standing problem in the Ca-ATPase field—the physical basis of the break (change in slope) in the Arrhenius plot of enzymatic activity, giving activation energies of approximately 12 and 20–28 kcal/mol above and below 20 °C, respectively (Inesi et al., 1973; Dean & Tanford, 1978; Bigelow et al., 1986; Squier et al., 1988b). This break has been proposed to originate from a change in the rate-limiting step of the reaction, a change in lipid fluidity, or a change in the conformation of the ATPase. Various physical methods have been used to determine whether the Arrhenius break is due to an abrupt change in the conformation of the

ATPase (Thomas & Hidalgo, 1978; Hoffmann et al., 1979; Burkli & Cherry, 1981; Andersen et al., 1981; Speirs et al., 1983; Bigelow et al., 1986). Saturation transfer EPR studies detected no discontinuity in the Arrhenius plot of the overall rotational motion of the Ca-ATPase (Squier et al., 1988b). The activation energy for protein mobility was identical with that of lipid fluidity (approximately 11 kcal/mol) and is higher than the activation energies of 7.4 ± 1.6, 7.9 ± 0.5, and 4.4 ± 0.7 kcal/mol calculated for $1/\phi_1$, $1/\phi_2$, and $1/\phi_3$ in our study. However, the Arrhenius plot calculated from the average rotational correlation time obtained from the single-exponential fit of the anisotropy decays in our study also gives an activation energy of 11.1 ± 0.5 kcal/mol (data not shown), in good agreement with the ST-EPR studies. The lack of time resolution in the ST-EPR studies prevented the determination of the separate correlation times, thus leading the authors to conclude that no abrupt change in the effective volume of the rotating protein unit occurs at or near 20 °C.

Transient absorption and phosphorescence studies of the Ca-ATPase have detected discontinuities in Arrhenius plots of anisotropy parameters, sometimes correlating with breaks in the Arrhenius plots of enzymatic activity. Hoffmann et al. (1979) observed a change in slope in the Arrhenius plot of a rotational rate parameter, with a similar slope below 15 °C and above 35 °C, and a plateau region from 15 to 35 °C. This was interpreted as a temperature-dependent change in the equilibrium between Ca-ATPase monomers and olgiomers, with increasing aggregation as the temperature is increased. However, signal-to-noise was low in this study, and the data were fit only to a single-exponential function, without allowing for either anisotropic motion or multiple motional species. Burkli and Cherry (1981) also observed discontinuities in the temperature dependence of both the rate and amplitude of motion, fitting the data to a single-exponential function plus a constant. The temperature dependence of an amplitude parameter showed a change in slope around 15–20 °C, with a plateau region above this temperature, in qualitative agreement with the present results (Figure 10). The authors suggested that this was due to increased aggregation at low temperatures. Energy transfer between a fluorescent lipid donor and an acceptor attached to the Ca-ATPase was observed to increase with temperature, suggesting disaggregation of the Ca-ATPase (Fagan & Dewey, 1986). The average radius of the oligomer in that study was calculated to be approximately 80 Å and was attributed to Ca-ATPase tetramers. Thus, the nonlinear temperature dependence of the apparent equilibrium constant between monomers and oligomers (Figure 11) is consistent with the temperature-dependent disaggregation of the ATPase proposed by Cherry and Godfrey (1981) and Fagan and Dewey (1986), but is in disagreement with the interpretation of Hoffmann et al. (1979).

The change in slope in the van't Hoff plot of the apparent dissociation constant $K = A_2/A_3$ may be important for understanding the temperature dependence of the Ca-ATPase reaction. The equilibrium constant of the proposed E_1 to E_2 conformational transition suggests that the E_2 conformation is stabilized at higher temperature (Inesi et al., 1973, 1976; Pick & Karlish, 1982). The temperature dependence of the equilibrium constant was found to be linear, with enthalpy changes of 12.5 kcal/mol (Inesi et al., 1976) and 20.5 kcal/mol (Pick & Karlish, 1982). These values are comparable to the value of 19 ± 2 kcal/mol obtained from the temperature dependence of K in the temperature range 4–20 °C in the present study (Figure 11). The E_1 to E_2 conformational transition was found to proceed with a large increase in entropy, 44 ± 2 cal mol^{-1} deg^{-1} (Inesi et al., 1976) and 65.6 cal mol^{-1} deg^{-1} (Pick & Karlish 1982), in agreement with the change in entropy of 66 ± 1 cal mol^{-1} deg^{-1} calculated for the apparent dissociation transition in the present study. Inesi et al. (1973) showed that the enthalpy of activation for calcium transport and Ca-ATPase activity is higher below 20 °C (27–30 kcal/mol) than above 20 °C (15–18 kcal/mol). The entropy of activation was found to be high and positive (34–40 cal mol^{-1} deg^{-1}) in the temperature range 5–20 °C, and negligible above 20 °C (0–4 cal mol^{-1} deg^{-1}), suggesting that enzymatic activity is limited by a highly ordered environment below 20 °C. This conclusion is also supported by other evidence that increased protein–protein interaction induced by cross-linking correlates well with reduced Ca-ATPase activity (Squier et al., 1988a). In summary, the correlation between the changes in enthalpy and entropy for the apparent dissociation of Ca-ATPase oligomers, found in the present study, with the changes in enthalpy and entropy for the E_1 to E_2 transition, provides evidence for the role of protein–protein interactions in limiting enzymatic activity.

Conclusions. The time-resolved phosphorescence anisotropy of ERITC-labeled SR reflects primarily the uniaxial rotational motion of the Ca-ATPase about the membrane normal. The results are all consistent with previous ST-EPR studies done under the same conditions, but the time resolution of the present study reveals new details about the complexity of the rotational motions. The anisotropy decay is heterogeneous, with several rotational species whose fractions vary with glycerol, ether, and temperature. The effects of glycerol are probability due to a direct effect on protein association due to dehydration, while those of ether and temperature may be mediated through lipid viscosity effects. For all three of these perturbations, there is a striking correlation between conditions that inhibit Ca-ATPase activity and those that promote protein association, especially the largest (slowest) of the aggregates. Analysis of the correlation times and amplitudes, along with the measured lipid viscosity, suggests that there are three major Ca-ATPase populations present from 4 to 40 °C, with the largest predominating at 4 °C, the intermediate one (probably a dimer) at 20 °C, and the smallest (probably a monomer) at 40 °C. The apparent interconversion of these components suggests temperature-dependent changes in the equilibrium between oligomeric and monomeric species of the Ca-ATPase, with protein association favored by low temperature and high lipid viscosity. We suggest that the breaks observed in the van't Hoff plot of the apparent dissociation constants at approximately 20 °C (Figure 11), and the break in the Arrhenius plot of Ca-ATPase activity observed at approximately the same temperature (Bigelow et al., 1986), share a common origin. That is, the increased enzymatic activity above 20 °C may be a manifestation of the change (a decrease) in protein–protein interaction, facilitated by a temperature-dependent conformational change in the Ca-ATPase polypeptide. The correlation between the changes in enthalpy and entropy for the E_1–E_2 transition and those obtained for the A_2–A_3 transition below 20 °C (Figure 11), suggests that below 20 °C, the rate-limiting step for enzymatic activity is controlled by ATPase–ATPase interactions. Further studies will be required to determine the structural bases of (a) the conformational change that leads to reduced protein–protein interaction with increasing temperature and (b) the oligomeric complexes that tend to form at low temperature.

Acknowledgments

We thank Mr. Robert Bennett for technical assistance in the construction and maintenance of the phosphorescence

instrumentation and Mr. Franz Nisswandt for technical assistance.

REFERENCES

Andersen, J. P., & Vilsen, B. (1985) *FEBS Lett. 189*, 13–17.
Andersen, J. P., Fellmann, P., Moller, J. V., & Devaux, P. F. (1981) *Biochemistry 20*, 4928–4936.
Bigelow, D. J., & Thomas, D. D. (1987) *J. Biol. Chem. 262*, 13449–13456.
Bigelow, D. J., Squier, T. C., & Thomas, D. D. (1986) *Biochemistry 25*, 194–202.
Birmachu, W., Nisswandt, F. L., & Thomas, D. D. (1989) *Biochemistry 28*, 3940–3947.
Brady, G. W., Fein, D. B., Harder, M. E., Spehr, R., & Meissner, G. (1981) *Biophys. J. 34*, 13–34.
Burkli, A., & Cherry, R. J. (1981) *Biochemistry 20*, 138–145.
Cherry, R. J. (1978) *Methods Enzymol. 54*, 47–61.
Cherry, R. J., & Godfrey, R. E. (1981) *Biophys. J. 36*, 257–276.
Dean, W. L., & Tanford, C. (1978) *Biochemistry 17*, 1683–1690.
Eads, T. M., Thomas, D. D., & Austin, R. H. (1984) *J. Mol. Biol. 179*, 55–81.
Fagan, M. H., & Dewey, T. G. (1986) *J. Biol. Chem. 261*, 3654–3660.
Franzini-Armstrong, C., & Ferguson, D. G. (1985) *Biophys. J. 48*, 607–615.
Herbette, L., DeFoord, P., Fleischer, S., Pascolinig, D., Scarpa, A., & Blasie, J. K. (1985) *Biochim. Biophys. Acta 817*, 103–122.
Hidalgo, C., Thomas, D. D., & Ikemoto, N. (1978) *J. Biol. Chem. 253*, 6879–6887.
Hoffman, W., Sarzala, M. G., & Chapman, D. (1979) *Proc. Natl. Acad. Sci. U.S.A. 76*, 3860–3864.
Hubbell, W. L., & McConnell, H. M. (1971) *J. Am. Chem. Soc. 93*, 314–326.
Hymel, L., Maurer, A., Berenski, C., Jung, C. Y., & Fleischer, S (1984) *J. Biol. Chem. 259*, 4890–4895.
Inesi, G., Millman, M., & Eletr, S. (1973) *J. Mol. Biol. 81*, 483–504.
Inesi, G., Cohen, J. A., & Coan, C. R. (1976) *Biochemistry 15*, 5293–5298.
Kawato, S., & Kinosita, K., Jr. (1981) *Biophys. J. 36*, 277–296.
Kinosita, K., Ishiwata, S., Yoshimura, H., Asai, H., & Ikegami, A. (1984) *Biochemistry 23*, 5963–5975.
Kutchai, H., & Campbell, K. P. (1989) *Biochemistry 28*, 4830–4839.
Laemmli, U. K. (1970) *Nature (London) 227*, 680–685.
Leberer, E., Charuk, J. H. M., Clarke, D. M., Green, N. M., Zubrzyckq-Gaarn, E., & MacLennan, D. H. (1989) *J. Biol. Chem. 264*, 3484–3493.
Lewis, S. M., & Thomas, D. D. (1986) *Biochemistry 25*, 4615–4621.
Lipari, G., & Szabo, A. (1980) *Biophys. J. 30*, 489–506.
Ludescher, R. D., & Thomas, D. D. (1988) *Biochemistry 27*, 3343–3351.
MacLennan, D. H., Brandl, C. J., Korczak, B., & Green, N. M. (1985) *Nature 316*, 696–700.
Martins, O. B., & de Meis, L. (1985) *J. Biol. Chem. 260*, 6776–6781.
Martonosi, A., Lagwiska, E., & Oliver, M. (1974) *Ann. N.Y. Acad. Sci. 227*, 549–557.
McIntosh, D. B., & Ross, D. C. (1988) *J. Biol. Chem. 263*, 12220–12223.
Mitchinson, C., Wilderspin, A. F., Trinnaman, B. J., & Green, N. M. (1982) *FEBS Lett. 146*, 87–92.
Napolitano, C. A., Cooke, P., Segalman, K., & Herbette, L. (1983) *Biophys. J. 42*, 119–125.
Pick, U., & Karlish, S. J. D. (1982) *J. Biol. Chem. 257*, 6120–6126.
Restall, C. J., Dale, R. E., Murray, E. K., Gilbert, C. W., & Chapman, D. (1984) *Biochemistry 23*, 6766–6776.
Saffman, P. J., & Delbrück, M. (1975) *Proc. Natl. Acad. Sci. U.S.A. 72*, 3111–3113.
Salama, G., & Scarpa, A. (1983) *Biochim. Biophys. Acta 32*, 3465–3477.
Silva, J. L., & Verjovski-Almeida, S. (1985) *J. Biol. Chem. 260*, 4764–4769.
Speirs, A., Moore, C. H., Boxer, D. H., & Garland, P. B. (1983) *Biochem. J. 213*, 67–74.
Squier, T. C., & Thomas, D. D. (1988) *J. Biol. Chem. 263*, 9171–9177.
Squier, T. C., & Thomas, D. D. (1989) *Biophys. J. 56*, 735–748.
Squier, T. C., Hughes, S. E., & Thomas, D. D. (1988a) *J. Biol. Chem. 263*, 9162–9170.
Squier, T. C., Bigelow, D. J., & Thomas, D. D. (1988b) *J. Biol. Chem. 263*, 9178–9186.
Taylor, K., Dux, L., & Martonosi, A. (1984) *J. Mol. Biol. 174*, 193–204.
Taylor, K. A., Mullner, N., Slawomir, P., Dux, L., Peracchia, C., Varga, S., & Martonosi, A. (1988) *J. Biol. Chem. 263*, 5287–5294.
Thomas, D. D. (1986) in *Techniques for the Analysis of Membrane Proteins* (Ragan, C. I., & Cherry, R. J., Eds.) pp 377–431, Chapman & Hall, New York.
Thomas, D. D., & Hidalgo, C. (1978) *Proc. Natl. Acad. Sci. U.S.A. 75*, 5488–5492.
Vanderkooi, J. M., Ierokomas, A., Nakamura, H., & Martonosi, A. (1977) *Biochemistry 16*, 1262–1267.
Van Winkle, W. B., Bick, R. J., Tate, C. A., & Entman, M. L. (1985) *Biophys. J. 47*, 2842a.
Vilsen, B., & Andersen, J. P. (1987) *Eur. J. Biochem. 170*, 421–429.
Worthington, C. R., & Liu, S. C. (1973) *Arch. Biochem. Biophys. 1578*, 573–579.